

# Chemical Cell-Surface Receptor Engineering Using Affinity-Guided, Multivalent Organocatalysts

Hangxiang Wang,<sup>†</sup> Yoichiro Koshi,<sup>†</sup> Daishiro Minato,<sup>†,‡</sup> Hiroshi Nonaka,<sup>†,§</sup> Shigeki Kiyonaka,<sup>†</sup> Yasuo Mori,<sup>†</sup> Shinya Tsukiji,<sup>||</sup> and Itaru Hamachi<sup>\*,†,⊥</sup>

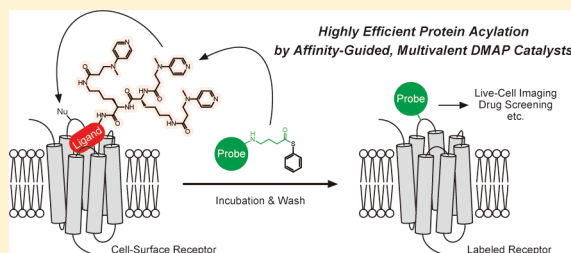
<sup>†</sup>Department of Synthetic Chemistry and Biological Chemistry, Graduate School of Engineering, Kyoto University, Katsura, Nishikyo-ku, Kyoto 615-8510, Japan

<sup>⊥</sup>Core Research for Evolutional Science and Technology (CREST), Japan Science and Technology Agency, 5 Sanbancho, Chiyoda-ku, Tokyo 102-0075, Japan

<sup>||</sup>Top Runner Incubation Center for Academia-Industry Fusion, Nagaoka University of Technology, 1603-1 Kamitomioka, Nagaoka, Niigata 940-2188, Japan

 Supporting Information

## ABSTRACT:



Catalysts hold promise as tools for chemical protein modification. However, the application of catalysts or catalyst-mediated reactions to proteins has only recently begun to be addressed, mainly in *in vitro* systems. By radically improving the affinity-guided DMAP (4-dimethylaminopyridine) (AGD) catalysts that we previously reported (Koshi, Y.; Nakata, E.; Miyagawa, M.; Tsukiji, S.; Ogawa, T.; Hamachi, I. *J. Am. Chem. Soc.* **2008**, *130*, 245.), here we have developed a new organocatalyst-based approach that allows specific chemical acylation of a receptor protein on the surface of live cells. The catalysts consist of a set of ‘multivalent’ DMAP groups (the acyl transfer catalyst) fused to a ligand specific to the target protein. It was clearly demonstrated by *in vitro* experiments that the catalyst multivalency enables remarkable enhancement of protein acylation efficiency in the labeling of three different proteins: congerin II, a Src homology 2 (SH2) domain, and FKBP12. Using a multivalent AGD catalyst and optimized acyl donors containing a chosen probe, we successfully achieved selective chemical labeling of bradykinin B<sub>2</sub> receptor (B<sub>2</sub>R), a G-protein coupled receptor, on the live cell-surface. Furthermore, the present tool allowed us to construct a membrane protein (B<sub>2</sub>R)-based fluorescent biosensor, the fluorescence of which is enhanced (tuned on) in response to the antagonist ligand binding. The biosensor should be applicable to rapid and quantitative screening and assay of potent drug candidates in the cellular context. The design concept of the affinity-guided, multivalent catalysts should facilitate further development of diverse catalyst-based protein modification tools, providing new opportunities for organic chemistry in biological research.

## INTRODUCTION

The ability to decorate specific proteins in a highly selective fashion with desired (unnatural) functionalities in cellular contexts is of great value in the study and control of living biological systems. Previous efforts have mainly focused on the development and use of engineered proteins in which a bioorthogonal moiety, such as unique peptide/protein tags and azide and alkyne groups, is genetically incorporated.<sup>1</sup> Selective labeling of the previously modified proteins is achieved in living cells using bioorthogonal chemical or enzymatic reactions. Alternatively, organic chemistry-based methods have also been developed, which typically use synthetic labeling reagents consisting of a specific protein ligand and a reactive (electrophilic) group.<sup>2–11</sup>

In this strategy, the ligand selectively binds to the target protein, driving a chemical reaction of the reactive group with an amino acid residue located on the protein surface through the proximity effect. The utmost advantage of this so-called “affinity labeling” is its applicability to specific modification of natural proteins without genetic engineering and without orthogonal reactions.<sup>2–9</sup> However, although several successful applications have been reported, the potential of organic chemistry-based approach in chemical protein labeling in cellular contexts has not yet been fully explored. In particular, chemical reactions and strategies

Received: May 14, 2011

Published: July 18, 2011

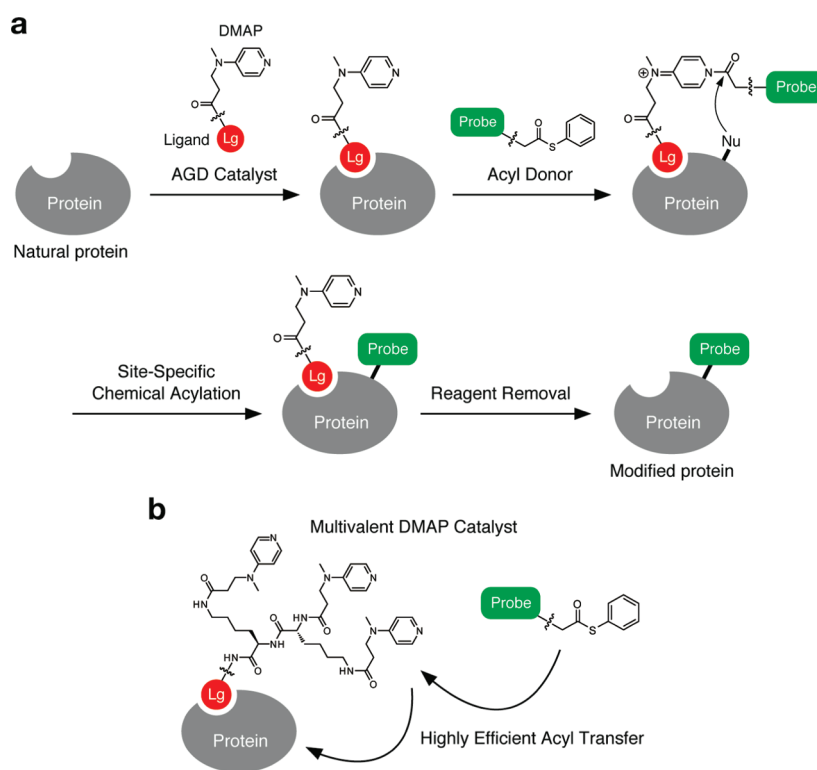


**Figure 1.** AGD catalyst-mediated selective chemical protein labeling. Schematic illustrations of (a) the basic strategy and (b) the present multivalent DMAP system. Lg, protein ligand; Nu, nucleophilic amino acid.

that can be used for protein surface modification remain very limited.

Catalysts have long played an essential role in organic synthesis, and thus hold promise as tools for chemical protein modification. However, the application of catalysts or catalyst-mediated reactions to protein engineering has only recently begun to be addressed.<sup>12–21</sup> To date, no reports have demonstrated the use of catalysts in selective chemical protein labeling in cellular contexts. The difficulty of designing molecular catalysts with high target selectivity and reaction efficiency that can function toward structurally complex biopolymers such as proteins in water-rich, heterogeneous environments represents a significant impediment.

DMAP is a representative organocatalyst which has been widely used for facilitating the acyl transfer reaction in a myriad of organic transformations.<sup>22</sup> We have recently shown that affinity-guided DMAP (AGD) catalysts consisting of the DMAP group and a saccharide ligand can be used for selective *in vitro* chemical acylation of lectins in combination with optimized, thiophenyl ester type of acyl donors (Figure 1a).<sup>23</sup> In this chemistry, the AGD catalyst selectively binds to the target protein, and the DMAP moiety mediates the transfer of the acyl group from the acyl donor to a nucleophilic amino acid located near the ligand-binding pocket. Therefore, this prototype of AGD catalyst has the advantages of target protein selectivity and reaction site specificity. However, the direct extension of this approach to live-cell systems was hampered by the slow reaction (see below). The development of a new strategy to enhance the reaction efficiency was necessitated.

Here, we describe an approach to remarkably improve the protein acylation efficiency using the AGD chemistry. Our approach is based on the introduction of an increased number of

DMAP groups into the AGD catalyst structure. In *in vitro* experiments, the multivalent AGD catalysts led to a significant enhancement of reaction rate and efficiency in the labeling of three different proteins: congerin II, a Src homology 2 (SH2) domain, and FKBP12. Taking advantage of the improved labeling properties, we carried out the covalent attachment of a synthetic fluorophore to bradykinin B<sub>2</sub> receptor (B<sub>2</sub>R), a G-protein coupled receptor, and constructed a membrane protein (B<sub>2</sub>R)-based fluorescent biosensor on the surface of live cells. To our knowledge, the ‘catalyst’ multivalency effect on enhanced reactivity is unprecedented. The design concept presented here is expected to facilitate further development of diverse catalyst-based protein modification tools.

## RESULTS AND DISCUSSION

**Design and *in Vitro* Evaluation of Affinity-Guided, Multivalent DMAP Catalysts.** The original AGD catalysts have proved to be applicable to selective protein (lectin) acylation,<sup>23</sup> but suffered from slow reaction rates. We hypothesized that increasing the number of DMAP catalysts within an AGD reagent might accelerate the reaction rate and efficiency of protein labeling (Figure 1b). This idea was inspired by the knowledge that binding affinity and specificity can be significantly enhanced by introducing multiple ligands into a molecule, known as the (ligand) multivalency effect.<sup>24,25</sup> First, to examine the validity of the multivalent catalyst strategy, we carried out *in vitro* labeling experiments using three different purified proteins: congerin II, the Src homology 2 (SH2) domain and FKBP12. AGD catalysts containing the corresponding specific ligand and a set of one, two, or three DMAP groups were designed and synthesized: compounds 1–3 for congerin II (ligand: lactose<sup>26</sup>); 4–6 for the SH2 domain

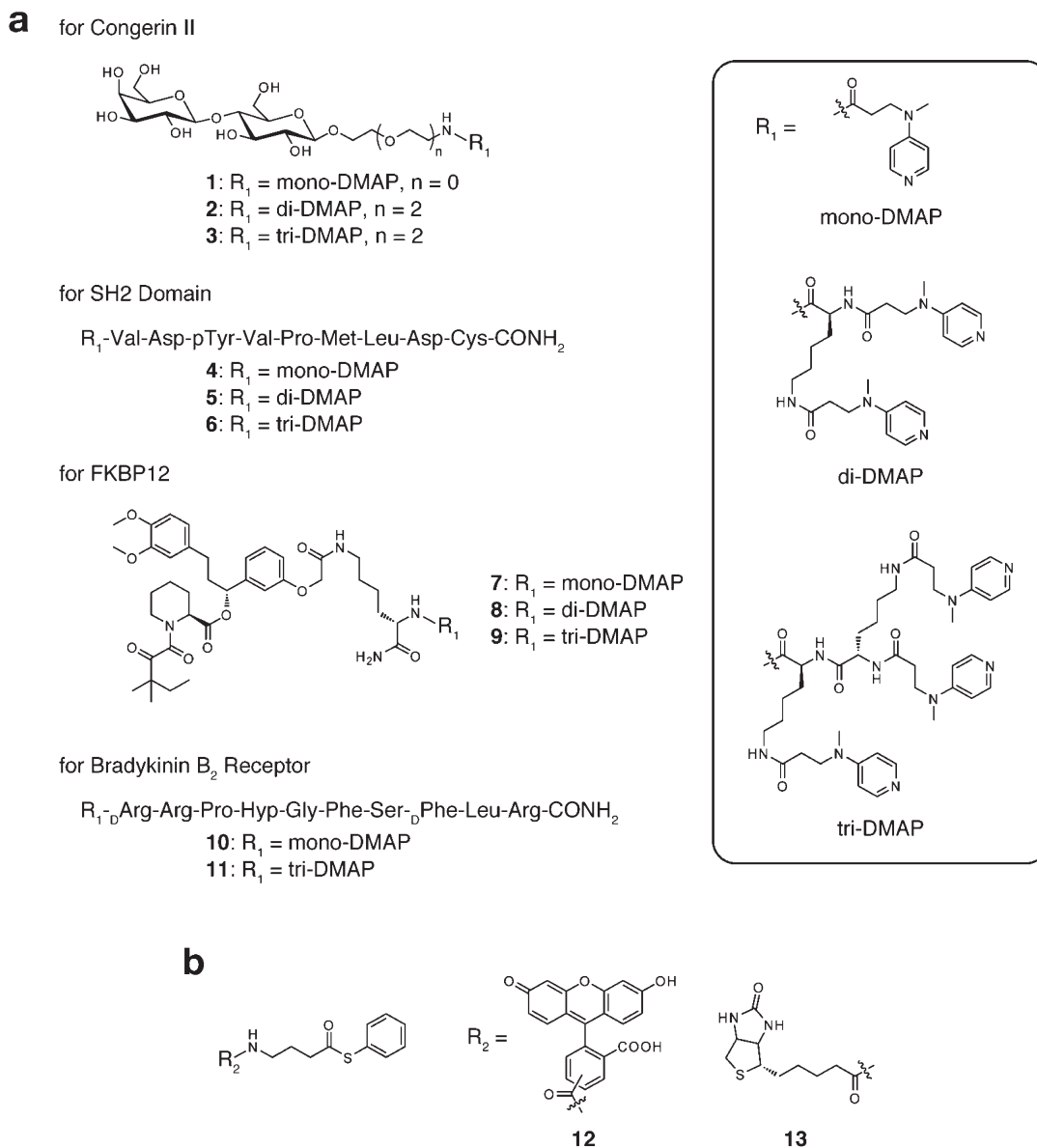


**Figure 2.** Chemical structures of (a) AGD catalysts and (b) acyl donors used in this study. 1–3 for congerin II, 4–6 for the SH2 domain derived from the p85 subunit of human phosphatidylinositol-3-kinase, 7–9 for FK506-binding protein 12 (FKBP12), and 10 and 11 for bradykinin B<sub>2</sub> receptor (B<sub>2</sub>R). Hyp, hydroxyproline.

(phosphotyrosine-containing peptide<sup>27</sup>); and 7–9 for FKBP12 (synthetic analogue of FK506<sup>28</sup>) (Figure 2a). We used previously optimized acyl donor 12 containing fluorescein<sup>23</sup> in the labeling experiments (Figure 2b). Labeling reactions were performed by incubating protein (10  $\mu$ M) with AGD catalyst (10  $\mu$ M) and acyl donor (50  $\mu$ M) in buffer, and monitored by MALDI-TOF mass spectrometry. As shown in Figure 3a and Figure S1, all of the protein targets were predominantly modified in a ratio of one fluorescein group per protein, irrespective of the DMAP valency. In addition, in all cases, no significant labeling occurred without AGD catalyst or in the presence of excess competitive ligand (Figure S2), which indicates that a specific protein–ligand interaction is required to drive the AGD-mediated protein acylation reaction. Of particular importance is the enhanced reactivity of multivalent AGD catalysts. As summarized in Figure 3b and Table S1, in the congerin II labeling, the initial rate of labeling was

accelerated with the increase of the number of DMAP moieties; by 3.6-fold for 2 (di-DMAP) and by 4.6-fold for 3 (tri-DMAP) compared to 1 (mono-DMAP). In the case of the SH2 domain, a more significant enhancement was observed (see also Figure 3c). Compounds 5 (di-DMAP) and 6 (tri-DMAP) accelerated the labeling reaction by 6.7-fold and 17.2-fold, respectively, compared to 4 (mono-DMAP). Similarly, 8 (di-DMAP) and 9 (tri-DMAP) showed 4.7-fold and 11.5-fold enhancement of FKBP12 labeling, respectively, relative to 7 (mono-DMAP) (see also Figure S3). It is noteworthy that the labeling of FKBP12 using tri-DMAP type 9 was very rapid and efficient, reaching approximately 90% labeling yield within 15 min.

We also determined the chemical modification sites. Peptide mapping analysis revealed that, in SH2 domain labeling, both the monovalent AGD catalyst 4 and its trivalent type 6 mediated specific acylation of a single residue, Lys379, which is an amino

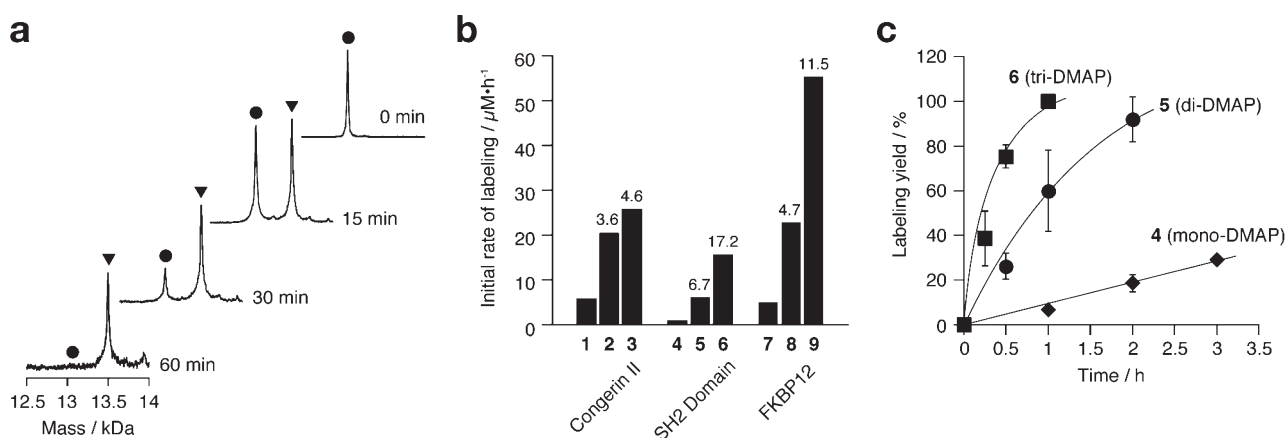


**Figure 3.** Improvement of chemical protein acylation efficiency by the DMAP multivalency effect. (a) Monitoring of the SH2 domain labeling processes by MALDI-TOF MS. Purified SH2 domain ( $10\ \mu\text{M}$ ) was incubated with AGD catalyst **6** ( $10\ \mu\text{M}$ ) and acyl donor **12** ( $50\ \mu\text{M}$ ) in buffer (pH 8.0) at  $25\ ^\circ\text{C}$ ; ●, unlabeled SH2 domain; ▼, fluorescein-labeled SH2 domain. (b) Initial rates of protein labeling using a series of AGD catalysts and **12**. Fold numbers are shown on the bars. (c) Reaction kinetics of the SH2 domain labeling using mono-, di-, and trivalent AGD catalysts.

acid proximal to the ligand binding pocket (Figure S4). This result indicates that the observed enhancement of labeling efficiency in the tri-DMAP system was not caused by changes in labeling pattern, such as the number and position of labeling sites. In the case of congerin II and FKBP12, the labeling also occurred at single sites: Tyr51<sup>23</sup> and Lys44 (Figure S5), respectively. These are each located near the ligand binding pocket of their proteins. To explore the mechanism of the multivalent DMAP effect, we first investigated whether the distance of the DMAP group from the affinity ligand, which differed among the mono-, di-, and trivalent catalysts, was related to labeling efficiency. Three different, monovalent AGD derivatives **14**, **15**, and **16** (for the SH2 domain) were used, in which a single DMAP was placed in a position corresponding to one of the three DMAP groups in trivalent AGD catalyst **6** (Figure S6). They showed almost no difference in labeling efficiency relative to the original type of monovalent AGD catalyst **4**. Next, we replaced one of the DMAP groups in divalent AGD catalysts with a triethylamine (TEA) derivative to examine the possible role of the second DMAP as a base. AGD catalysts **17** (for the SH2 domain) and **18** (for FKBP12) possessing one DMAP and one TEA group accelerated the labeling reaction by 3.7-fold and 2.4-fold, respectively, compared to the parental, monovalent AGD catalysts that do not contain the TEA moiety (**4** and **7**, respectively) (Figure S7). The labeling efficiencies observed with **17** and **18** were intermediate between those with monovalent and divalent DMAP counterparts (**4** and **5**, and **7** and **8**, respectively). Although the exact mechanism is not yet fully understood, it is very likely that some DMAPs within multivalent AGD catalysts act not only as an activator, but also partially as a base to accelerate the acyl transfer reaction. Thus, the activator DMAP increases the reactivity of the acyl donor via formation of an *N*-acylpyridinium intermediate, and the DMAP base may assist the deprotonation of other DMAP(s) and/or a nucleophilic amino acid residue targeted for labeling (e.g., lysine and tyrosine). Overall, incorporating a set of multiple DMAP groups into an AGD catalyst was demonstrated to dramatically enhance the efficiency of the protein acylation reaction.

**Selective Chemical Labeling of B<sub>2</sub>R on the Surface of Live Cells.** Having proved the efficacy of multivalent AGD catalysts, we were motivated to apply the strategy to chemical modification of cell-surface proteins in the context of living cells. Bradykinin B<sub>2</sub>

receptor (B<sub>2</sub>R), a G protein-coupled receptor (GPCR), was chosen as the first target protein. We used the B<sub>2</sub>R-selective antagonist peptide,  $\text{DArg}^8[\text{Hyp}^3, \text{D}^7\text{Phe}, \text{Leu}^8]\text{BK}$ ,<sup>29</sup> as a specific ligand and synthesized AGD catalyst **11** containing three DMAP groups (Figure 2a). Human embryonic kidney (HEK) 293 cells transfected with human B<sub>2</sub>R were used in the experiments. After washing twice with HBS buffer, the cells were incubated in the buffer with **11** ( $10\ \mu\text{M}$ ) and the cell-membrane impermeable fluorescein-type acyl donor **12** ( $20\ \mu\text{M}$ ) at  $37\ ^\circ\text{C}$  for 30 min. Subsequently, the cells were washed to remove the catalyst and unreacted acyl donor and observed by confocal laser scanning microscopy (CLSM). As shown in Figure 4a, a strong fluorescence signal was detected in the periphery of the cells. To examine the possibility of nonspecific labeling, we incubated the cells with **11** and **12** in the presence of excess HOE 140 (Table S2),<sup>30</sup> a strong inhibitor of B<sub>2</sub>R, or with **12** alone (no catalyst). In neither case was fluorescence observed. Therefore, it was concluded that the fluorescence detected was due to fluorescein labeling of B<sub>2</sub>R at the cell surface. We also attempted to modify B<sub>2</sub>R with a biotin tag using acyl donor **13**<sup>23</sup> (Figure 2b). After performing the reaction as described above, the cells were washed, lysed, and analyzed by Western blotting. Using anti-B<sub>2</sub>R antibody and streptavidin–horseradish peroxidase conjugate (SAv-HRP), we detected only a single major band corresponding to biotinylated B<sub>2</sub>R (Figure 4b). This band was not present when the labeling was carried out in the presence of excess HOE 140 or in the absence of **11**. Taken together, these results verify that the seven membrane-spanning B<sub>2</sub>R can be modified covalently and selectively with synthetic functional molecules via **11**-catalyzed acyl transfer reaction. No significant change in the cell morphology occurred throughout the labeling processes, indicating the biocompatibility of this method.

Kinetic experiments showed that fluorescein labeling of B<sub>2</sub>R reached a plateau at around 30 min, at which time the labeling yield was estimated to be approximately 85% of the entire cell-surface population of B<sub>2</sub>R (Figure 4c). In sharp contrast, the mono-DMAP type of AGD catalyst (**10**) gave only a negligible level of fluorescein labeling even after 60 min incubation. This result demonstrates that the DMAP multivalency is essential to achieve cell-surface B<sub>2</sub>R labeling. Furthermore, we confirmed that the AGD-mediated modification did not impair the natural



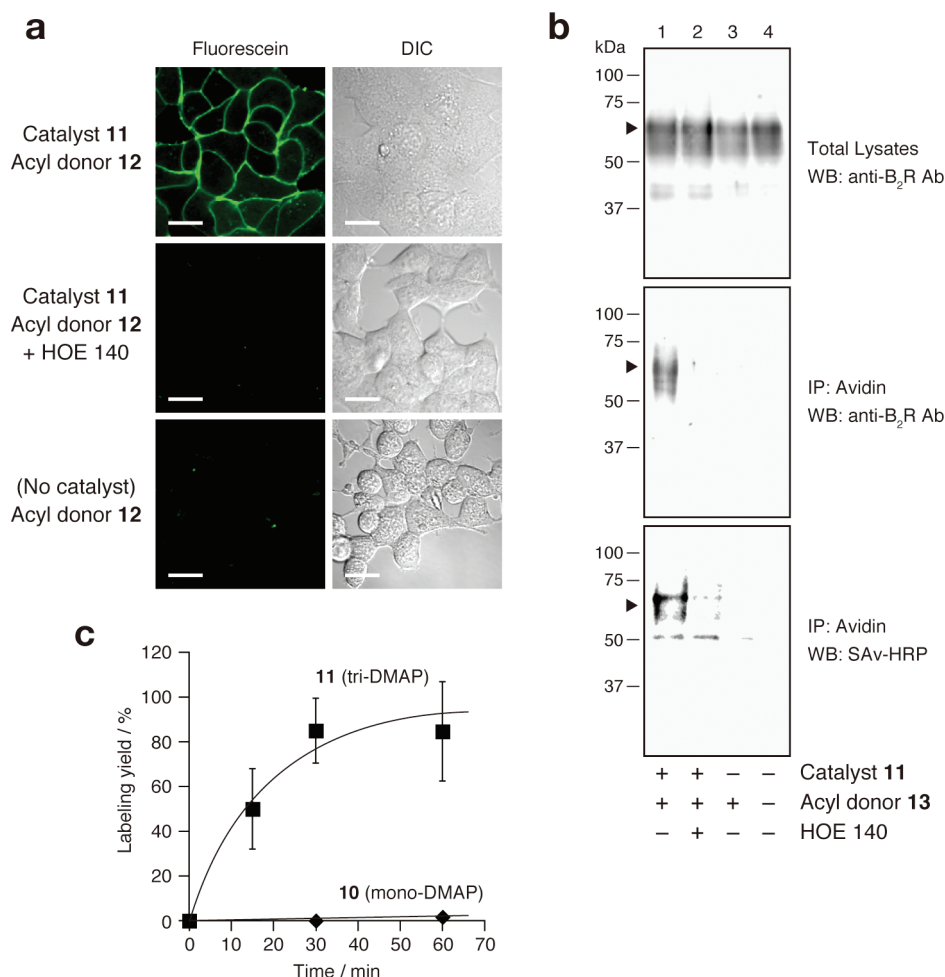


**Figure 4.** Specific labeling of cell-surface B<sub>2</sub>R on living cells using AGD chemistry. (a) Fluorescein labeling. HEK 293 cells transfected with B<sub>2</sub>R were treated with trivalent AGD catalyst **11** (10  $\mu$ M) and acyl donor **12** (20  $\mu$ M) for 30 min at 37 °C in HBS buffer (pH 8.0) (top). As negative controls, the labeling reaction was performed in the presence of HOE 140 (10  $\mu$ M) (center) or without **11** (bottom). After washing, the cells were observed by CLSM. Scale bars, 10  $\mu$ m. (b) Biotin labeling. Labeling reactions were performed as described in panel a using acyl donor **13**. After washing, the cells were lysed and analyzed by Western blotting. The arrowhead indicates B<sub>2</sub>R, which is observed as a broad band. (c) Comparison of the efficiency of the cell-surface B<sub>2</sub>R labeling using monovalent and trivalent AGD catalysts (**10** and **11**, respectively). Labeling reactions were performed as described in panel a, and the cells were washed at indicated time points and observed by CLSM. The labeling efficiency was determined as described in the Experimental Section.

function of B<sub>2</sub>R. The agonist-induced increase in intracellular Ca<sup>2+</sup> concentration was measured using fura-2. Bradykinin-stimulated Ca<sup>2+</sup> signaling activity was essentially identical before and after fluorescein labeling (Figure S8). In addition, the present labeling method was applicable not only in buffer, but also in cell culture medium both with and without serum (data not shown).

**Construction of a GPCR-Based Semisynthetic Fluorescent Biosensor.** Owing to their critical roles in diverse physiological and pathological processes, the GPCR family is now one of the most important target classes for drug discovery.<sup>31</sup> Few convenient, quantitative and direct methods have been developed for the evaluation of GPCR–ligand interactions as a means of identifying drug candidates. Given the success of fluorescent labeling of B<sub>2</sub>R using AGD chemistry (see above), we sought to construct a GPCR-based semisynthetic biosensor that responds to specific ligands with ‘turn-on’ fluorescence (Figure 5a). Our strategy uses the bimolecular fluorescence quenching and recovery (BFQR) mechanism.<sup>9,32</sup> Taking advantage of the straightforward removal of AGD catalyst **11** by a simple washing procedure (Figure S9),

the fluorescein-modified B<sub>2</sub>R (Fl-B<sub>2</sub>R) in an unliganded state was constructed on the surface of HEK293 cells. A B<sub>2</sub>R antagonist peptide ligand conjugated with the 4-dimethylaminophenylazobenzene-4-carboxylic acid (DABCYL) quencher (**19**) (1  $\mu$ M) was added to the culture medium and induced a significant decrease in the Fl-B<sub>2</sub>R-derived fluorescence in a typical saturation behavior, generating a quenched state of Fl-B<sub>2</sub>R. (Figure 5b–d and Figure S10). Subsequently, the addition of HOE 140 (2  $\mu$ M; reported K<sub>D</sub> for human B<sub>2</sub>R, 0.41 nM (ref 30)) resulted in a substantial recovery of fluorescence. In contrast, almost no fluorescence change was observed by the addition of saralasin,<sup>33</sup> an antagonist of the angiotensin II receptor (Figure 5e and Figure S11). These observations are fully consistent with the proposed BFQR scheme shown in Figure 5a, and demonstrate that the fluorescence recovery induced by HOE 140 was due to the displacement of the noncovalently bound antagonist–DABCYL conjugate **19** from the Fl-B<sub>2</sub>R. This BFQR-based turn-on fluorescence assay system allowed us to evaluate the (relative) affinities of various ligands in a simple manner. B9430 (Table S2;

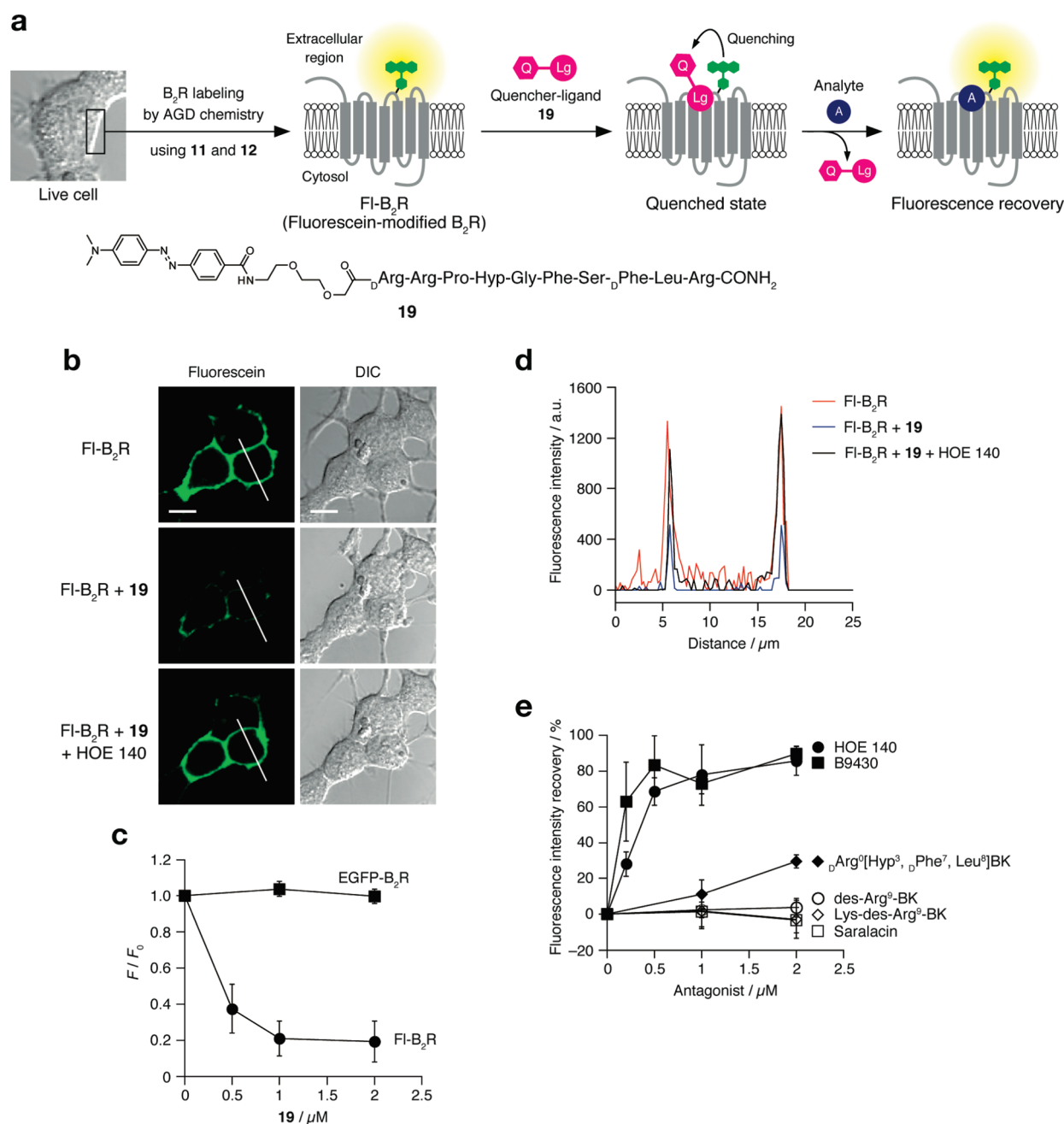


**Figure 5.** Construction of B<sub>2</sub>R-based fluorescent biosensor on the basis of the BFQR mechanism. (a) Schematic illustration of the strategy. (b) Fluorescence quenching and recovery of FI-B<sub>2</sub>R observed by CLSM. Postlabeled HEK293 cells (top) were treated with DABCYL-appended B<sub>2</sub>R antagonist **19** (1  $\mu$ M) (center), which was followed by the addition of HOE 140 (2  $\mu$ M) (bottom). Scale bars, 10  $\mu$ m. (c) Quantitative evaluation of fluorescence intensity changes of FI-B<sub>2</sub>R and EGFP-B<sub>2</sub>R upon the addition of **19**. (d) Fluorescence intensities (arbitrary units) along the white lines shown in images in panel b. (e) Quantitative fluorescence detection of various B<sub>2</sub>R ligands with the FI-B<sub>2</sub>R biosensor. To the quenched state of FI-B<sub>2</sub>R prepared as described in panel b was added each B<sub>2</sub>R ligand.

reported  $K_D$ , 0.25 nM (ref 30)), another high-affinity antagonist, potently restored fluorescence, and  $\text{D}^0\text{Arg}^0[\text{Hyp}^3, \text{D}^0\text{Phe}^7, \text{Leu}^8]\text{BK}$  (reported  $K_D$ , 2.8 nM (ref 29)) induced a moderate but significant change (Figure 5e). On the other hand, the FI-B<sub>2</sub>R biosensor did not respond to des-Arg<sup>9</sup>-BK and Lys-des-Arg<sup>9</sup>-BK (Table S2; reported  $K_D$ , 8.1  $\mu$ M and >30  $\mu$ M, respectively<sup>30</sup>), both of which are low-affinity ligands. The relative order of affinity of the ligands assessed using the BFQR system was in good agreement with that reported previously. Therefore, we have

demonstrated that the fluorophore-labeled B<sub>2</sub>R can function as a turn-on fluorescent biosensor for various antagonist candidates.

As an intriguing comparison, we also attempted to construct a similar BFQR-based biosensor system using a conventional genetic technique. The B<sub>2</sub>R was fluorescently labeled by fusing enhanced green fluorescent protein (EGFP) to its N-terminus (EGFP-B<sub>2</sub>R). HEK 293 cells expressing EGFP-B<sub>2</sub>R displayed fluorescence predominantly in the periphery of the cells (Figure S10). However, in contrast to the above FI-B<sub>2</sub>R system, no quenching

of EGFP fluorescence took place upon the addition of **19** (Figure S5 and Figure S10), suggesting that the distance between the quencher and the EGFP moiety was too great. This highlights the advantage of the present AGD-based method in which a small fluorophore is installed close to the ligand binding pocket of the target protein.

## CONCLUSION

Introducing multiple DMAP groups into AGD catalysts has proven a powerful strategy to achieve efficient, selective chemical acylation of proteins under mild and biocompatible conditions. While the effect of ligand multivalency on molecular recognition has been intensively studied,<sup>24,25</sup> the 'catalyst' multivalency effect on enhanced reactivity described here is, to our knowledge, unprecedented. Besides the high target selectivity imposed by the affinity guidance, the enhanced labeling efficiency induced by the catalyst multivalency was essential for modifying and engineering a specific membrane-spanning receptor with synthetic probes on the live cell surface. In recent decades, chemists have developed a variety of organocatalysts for environmentally benign chemical processes.<sup>34</sup> The present study demonstrates the first successful application of organocatalysts to (selective) biopolymer modification in cellular contexts. In general, organocatalysts should be less toxic and highly tolerant to a wide range of functionalities found in biological environments. The catalyst multivalency along with the affinity-guidance strategy may be of key importance in utilizing organocatalysts for chemical biopolymer labeling, imaging and engineering in the context of biological systems.

## EXPERIMENTAL SECTION

**Synthesis.** All synthetic procedures and compound characterizations are described in the Supporting Information.

**General Materials and Methods.** Unless otherwise noted, all proteins/enzymes and reagents were obtained from commercial suppliers (Sigma, Aldrich, Tokyo Chemical Industry (TCI), or Wako Pure Chemical Industries) and used without further purification. UV–visible spectra were recorded on a Shimadzu UV-2550 spectrophotometer. SDS–polyacrylamide gel electrophoresis (SDS–PAGE) and Western blotting were carried out using a Bio-Rad Mini-Protein III electrophoresis apparatus. Analytical RP–HPLC was carried out on a Hitachi LaChrom L-7100 system equipped with LaChrom L-7400 UV and L-7485 fluorescence detectors, and a YMC-Pack ODS-A column (5  $\mu$ m, 250  $\times$  4.6 mm) at a flow rate of 1.0 mL/min. UV detection was at 220 nm and fluorescence detection was at 515 nm with excitation at 480 nm. All runs used linear gradients of acetonitrile containing 0.1% TFA (solvent A) and 0.1% aqueous TFA (solvent B). MALDI–TOF MS spectra were recorded on an Autoflex II instrument (Bruker Daltonics) using  $\alpha$ -cyano-4-hydroxycinnamic acid (CHCA) or sinapinic acid (SA) as the matrix. Cell imaging was performed with a confocal laser scanning microscope (CLSM, Olympus, FV1000, IX81) equipped with a 100 $\times$ , NA = 1.40 oil objective. Fluorescence images were acquired using the 351 nm line of an argon laser for excitation of Hoechst 33342 (emission detection range, 400–470 nm), the 488 nm line of an argon laser for excitation of fluorescein and EGFP (emission, 500–600 nm) and the 633 nm line of a HeNe Red laser for excitation of Cy5 (emission, 645–745 nm). The chemiluminescence signal using Chemi-Lumi one (Nacalai Tesque) was detected with a LAS 4000 imaging system (Fuji Film).

**Congerin II Labeling.** Recombinant congerin II was expressed in *Escherichia coli* strain JM109/pTV-Con II and purified as previously described.<sup>35</sup> Purified congerin II (10  $\mu$ M) was incubated with acyl donor **12** (50  $\mu$ M) in the presence of AGD catalyst **1**, **2**, or **3** (10  $\mu$ M) in

HEPES buffer (50 mM, pH 8.0) at 25  $^{\circ}$ C. Control reactions in the presence of excess lactose (100 equiv) or without catalyst were also carried out. Aliquots at different time points were taken, and the labeling yields were determined by MALDI–TOF MS (SA).

**SH2 Domain Labeling.** Recombinant human SH2 domain was obtained as described previously.<sup>9</sup> Purified SH2 domain (10  $\mu$ M) was incubated with acyl donor **12** (50  $\mu$ M) in the presence of AGD catalyst **4**, **5**, or **6** (10  $\mu$ M) in HEPES buffer (50 mM, pH 8.0) at 25  $^{\circ}$ C. Control labeling reactions in the presence of excess peptide ligand (100 eq, AcHN-VDpYVPMLD-CONH<sub>2</sub>) or without catalyst were also carried out. Aliquots at different time points were taken, and the labeling yields were determined by MALDI–TOF MS (SA). Labeling reactions with AGD derivatives **14**–**17** were performed under the same condition.

**FKBP12 Labeling.** Recombinant human FKBP12 was obtained as described previously.<sup>8</sup> Purified FKBP12 (10  $\mu$ M) was incubated with acyl donor **12** (50  $\mu$ M) in the presence of AGD catalyst **7**, **8**, or **9** (10  $\mu$ M) in Tris buffer (50 mM, pH 8.0) at 37  $^{\circ}$ C. Control labeling reactions in the presence of excess FK506 (10 equiv) or without catalyst were also carried out. Aliquots at different time points were taken, and the labeling yields were determined by MALDI–TOF MS (SA). Labeling reactions with AGD derivative **18** were performed under the same condition.

**Peptide Mapping of the Fluorescein-Labeled SH2 Domain.** Labeling was performed under the following condition: 17  $\mu$ M SH2 domain, 17  $\mu$ M AGD catalyst **4** or **6**, 85  $\mu$ M fluorescein acyl donor **12** in 50 mM HEPES (pH 8.0) at 25  $^{\circ}$ C. The labeled SH2 domain was purified by semipreparative RP–HPLC. The fraction containing the labeled SH2 domain was collected and dialyzed against HEPES buffer (50 mM, pH 8.0) with a Spectra/Por dialysis membrane (MWCO: 3,000). The resulting solution was concentrated using a Centricon Ultracel YM-3 (Millipore). To this solution, urea (at a final concentration of 2 M) and trypsin (trypsin/substrate ratio = 1/10 (w/w)) were added. After incubation at 37  $^{\circ}$ C overnight, the digested peptides were separated by analytical RP–HPLC. The collected fractions were analyzed by MALDI–TOF MS (CHCA) and the labeled fragment was further characterized by MALDI–TOF MS/MS analysis.

**Peptide Mapping of the Fluorescein-Labeled FKBP12.** Labeling was performed under the following condition: 20  $\mu$ M FKBP12, 20  $\mu$ M AGD catalyst **9**, 40  $\mu$ M fluorescein acyl donor **12** in Tris buffer (50 mM, pH 8.0) at 37  $^{\circ}$ C. The labeled FKBP12 was purified by semipreparative RP–HPLC. The fraction containing the labeled FKBP12 was collected and dialyzed against HEPES buffer (50 mM, pH 8.0) with a Spectra/Por dialysis membrane (MWCO: 3,000). The resulting solution was concentrated using a Centricon Ultracel YM-3 (Millipore). To this solution, urea (at a final concentration of 2 M) and lysyl endopeptidase (LEP) (LEP/substrate ratio = 1/10 (w/w)) were added. After incubation at 37  $^{\circ}$ C overnight, the digested peptides were separated by analytical RP–HPLC. The collected fractions were analyzed by MALDI–TOF MS (CHCA) and the labeled fragment was further characterized by MALDI–TOF MS/MS analysis.

**Construction of the Expression Plasmid for  $\alpha$ 7-FLAG-Fused B<sub>2</sub>R.** An oligo DNA fragment coding the FLAG tag sequence was inserted into *Xho*I–*Bam*HI sites of pBS-B<sub>2</sub>R (ref 36) to yield pBS-FLAG-B<sub>2</sub>R. The sequences of the 5'-phosphorylated DNA fragments were as follows: forward (5'-TCGAGGAAGCTTGGACTACAAGGACGATGACGACAAG-3'), reverse (5'-GATCCTTGTCGTCATC-GTCCTTGTAGTCCAAGCTTCC-3'). An oligo DNA fragment coding the N-terminal sequence of  $\alpha$ 7 nicotinic acetylcholine receptor, a signal sequence for plasma membrane transportation, was inserted into *Xho*I site of pBS-FLAG-B<sub>2</sub>R to yield pBS- $\alpha$ 7-FLAG-B<sub>2</sub>R. The sequences of the 5'-phosphorylated DNA fragments were as follows:  $\alpha$ 7-1(+) (5'-TCGAGCCACCATGGGCTCCGGGCGCTGATGCTGTGG-CTGCTGGCGGCGG-3'),  $\alpha$ 7-2(+) (5'-CGGGGCTCGTGCGCGA-GTCCCTGCAAGGAGAGTTCCAAAGGAAGCTGTACAAGGA-3'),



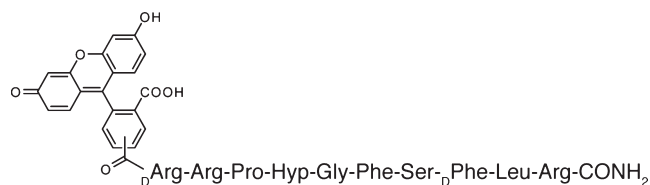
$\alpha$ -7-1(–) (5′-TCGATCCTTGACAGCTTCCTTTGGAAGCTCTCC-TTGACGGGACTCGCGACGA-3′) and  $\alpha$ -7-2(–) (5′-GCCCCGCC-GCCGCCAGCAGCCACAGCATCAGCGCCCGGAGGCCCATGG-TGGC-3′). An *XhoI*–*EcoRI* fragment of pBS- $\alpha$ 7-FLAG-B<sub>2</sub>R was inserted into the same digestion site of pCI-neo plasmid (Promega) to yield pCI- $\alpha$ 7-FLAG-B<sub>2</sub>R.

**Construction of the Expression Plasmid for EGFP-Fused B<sub>2</sub>R.** An EGFP fragment was obtained by PCR from pEGFP-N1 (Clontech) using a pair of primers, forward (5′-AGGATCCAATGGT-GAGCAAGGGCGAGGAGC-3′) and reverse (5′-TGGATCCGCCT-TGTACAGCTCGTCCATGCC-3′), and subcloned into the *Bam*HI site of pBS- $\alpha$ 7-FLAG-B<sub>2</sub>R to yield pBS- $\alpha$ 7-FLAG-EGFP-B<sub>2</sub>R. An *XhoI*–*EcoRI* fragment from pBS- $\alpha$ 7-FLAG-EGFP-B<sub>2</sub>R was inserted into pCI-neo plasmid (Promega) to yield pCI-EGFP-B<sub>2</sub>R.

**Fluorescein Labeling of B<sub>2</sub>R and the BFQR Assay on the Surface of HEK 293 Cells.** HEK 293 cells stably expressing human B<sub>2</sub>R fused to an  $\alpha$ 7-FLAG sequence were maintained in DMEM with 10% fetal bovine serum (FBS), penicillin (100 units/mL), and streptomycin (100  $\mu$ g/mL) at 37 °C and 5% CO<sub>2</sub>. Before labeling, the cells were washed twice with HBS buffer (107 mM NaCl, 6 mM KCl, 1.2 mM MgSO<sub>4</sub>, 2 mM CaCl<sub>2</sub>, 11.5 mM glucose, 20 mM HEPES, pH 8). Labeling was conducted in HBS buffer containing AGD catalyst **10** or **11** (10  $\mu$ M) and acyl donor **12** (20  $\mu$ M) for 30 min at 37 °C. As control, the labeling experiments in the presence of HOE 140 (10  $\mu$ M) or in the absence of catalyst **11** were also conducted. After labeling, the cells were washed with HBS buffer three times to remove the unreacted acyl donor and catalyst. The cells were then observed by CLSM. The BFQR assay using quencher-ligand **19** was performed as described in the corresponding figure captions.

To estimate the fluorescein labeling efficiency, we used fluorescein-modified B<sub>2</sub>R ligand **20** as a fluorescent marker. After labeling and washing procedures, the fluorescence intensity of the labeled, cell-surface B<sub>2</sub>R ( $F_{\text{label}}$ ) was measured by CLSM. Subsequently, **20** was added to the cell culture medium (at a final concentration of 1  $\mu$ M) to stain the whole cell-surface B<sub>2</sub>R, and the total fluorescence intensity ( $F_{\text{total}}$ ) was measured. The labeling efficiency was then determined by the eq 1:

$$\text{Labeling efficiency (\%)} = F_{\text{label}} / (F_{\text{total}} - F_{\text{label}}) \times 100 \quad (1)$$



**20**

**Biotin Labeling of B<sub>2</sub>R.** Biotin labeling was carried out as described above using AGD catalyst **11** (10  $\mu$ M) and acyl donor **13** (10  $\mu$ M) for 30 min at 37 °C. After washing, the cells were collected and lysed with RIPA lysis buffer (pH 7.6, 25 mM Tris, 150 mM NaCl, 0.1% SDS, 1% Nonidet P-40, 1% Deoxycholic acid) containing 1% protease inhibitor cocktail set III (Novagen) at 4 °C for 30 min. After centrifugation, the supernatant was recovered. The biotinylated B<sub>2</sub>R was purified by SoftLink Soft Release Avidin Resin (Promega) and eluted with 5 mM biotin in RIPA buffer according to the manufacturer's protocol. The eluent was mixed with 2 $\times$  sample buffer (pH 6.8, 125 mM Tris·HCl, 20% Glycerol, 4% SDS, 0.01% Bromophenol blue, 100 mM DTT). The samples were resolved by 10% SDS–PAGE and electrotransferred onto an Immun-Blot PVDF membrane (Bio-Rad). The biotinylated product was detected with streptavidin–horseradish peroxidase conjugate (SAV-HRP, Invitrogen) using Chemi-Lumi One (Nacalai Tesque). The immunodetection of B<sub>2</sub>R was performed

with anti-B<sub>2</sub>R antibody and anti-rabbit IgG-HRP conjugate (both Santa Cruz Biotechnology).

**Evaluation of the B<sub>2</sub>R-Mediated Ca<sup>2+</sup> Influx Activity.** The B<sub>2</sub>R-mediated Ca<sup>2+</sup> influx activity was measured according to the method previously reported.<sup>37</sup> HEK 293 cells transiently expressing B<sub>2</sub>R were plated onto poly-L-lysine-coated glass coverslips. B<sub>2</sub>R labeling was carried out using AGD catalyst **11** and acyl donor **12** as described above. The postlabeled cells were added with 1  $\mu$ M Fura-2/AM (Dojindo) and incubated at 37 °C for 40 min in HBS buffer (pH 7.4, containing 2 mM Ca<sup>2+</sup>). The coverslips were set in a perfusion chamber mounted on the stage of the microscope. One micromolar bradykinin, the B<sub>2</sub>R agonist, was applied to the cells by perfusion as a stimulus of B<sub>2</sub>R-mediated Ca<sup>2+</sup> signaling. Fluorescence changes of Fura-2 inside the cells were recorded and analyzed with a video image analysis of system (Aqua Cosmos; Hamamatsu Photonics). As control, HEK 293 cells transfected with pCI-neo vector were subjected to the Ca<sup>2+</sup> measurement.

## ■ ASSOCIATED CONTENT

**S Supporting Information.** Figures S1–S11, Tables S1–S2, and experimental details of the synthesis. This material is available free of charge via the Internet at <http://pubs.acs.org>.

## ■ AUTHOR INFORMATION

### Corresponding Author

ihamachi@sbchem.kyoto-u.ac.jp

### Present Addresses

<sup>†</sup>Graduate School of Medicine and Pharmaceutical Sciences, University of Toyama, 2630 Sugitani, Toyama 930-0194, Japan.

<sup>§</sup>INAMORI Frontier Research Center, Kyushu University, 744 Motooka, Nishi-ku, Fukuoka 819-0395, Japan.

## ■ ACKNOWLEDGMENT

We thank Dr. Tomohisa Ogawa (Tohoku University) for the *E. coli* strain JM109/pTV-Con II. Y.K. and H.N. acknowledge the Japan Society for the Promotion of Science Research Fellowships for Young Scientists.

## ■ REFERENCES

- (1) Sletten, E. M.; Bertozzi, C. R. *Angew. Chem., Int. Ed.* **2009**, *48*, 6974–6998.
- (2) Wold, F. *Methods Enzymol.* **1977**, *46*, 3–14.
- (3) Hamachi, I.; Nagase, T.; Shinkai, S. *J. Am. Chem. Soc.* **2000**, *122*, 12065–12066.
- (4) Chen, G.; Heim, A.; Riether, D.; Yee, D.; Milgrom, Y.; Gawinowicz, M. A.; Sames, D. *J. Am. Chem. Soc.* **2003**, *125*, 8130–8133.
- (5) Takaoka, Y.; Tsutsumi, H.; Kasagi, N.; Nakata, E.; Hamachi, I. *J. Am. Chem. Soc.* **2006**, *128*, 3273–3280.
- (6) Harvey, J. H.; Trauner, D. *ChemBioChem* **2008**, *9*, 191–193.
- (7) Fortin, D. L.; Banghart, M. R.; Dunn, T. W.; Borges, K.; Wagenaar, D. A.; Gaudry, Q.; Karakossian, M. H.; Otis, T. S.; Kristan, W. B.; Trauner, D.; Kramer, R. H. *Nat. Methods* **2008**, *5*, 331–338.
- (8) Tsukiji, S.; Miyagawa, M.; Takaoka, Y.; Tamura, T.; Hamachi, I. *Nat. Chem. Biol.* **2009**, *5*, 341–343.
- (9) Tsukiji, S.; Wang, H.; Miyagawa, M.; Tamura, T.; Takaoka, Y.; Hamachi, I. *J. Am. Chem. Soc.* **2009**, *131*, 9046–9054.
- (10) Volgraf, M.; Gorostiza, P.; Numano, R.; Kramer, R. H.; Isacoff, E. Y.; Trauner, D. *Nat. Chem. Biol.* **2006**, *2*, 47–52.
- (11) Gorostiza, P.; Volgraf, M.; Numano, R.; Szobota, S.; Trauner, D.; Isacoff, E. Y. *Proc. Natl Acad. Sci. U.S.A.* **2007**, *104*, 10865–10870.
- (12) Antos, J. M.; Francis, M. B. *J. Am. Chem. Soc.* **2004**, *126*, 10256–10257.



- (13) McFarland, J. M.; Francis, M. B. *J. Am. Chem. Soc.* **2005**, *127*, 13490–13492.
- (14) Ojida, A.; Tsutsumi, H.; Kasagi, N.; Hamachi, I. *Tetrahedron Lett.* **2005**, *46*, 3301–3305.
- (15) Tilley, S. D.; Francis, M. B. *J. Am. Chem. Soc.* **2006**, *128*, 1080–1081.
- (16) Kodama, K.; Fukuzawa, S.; Nakayama, H.; Kigawa, T.; Sakamoto, K.; Yabuki, T.; Matsuda, N.; Shirouzu, M.; Takio, K.; Tachibana, K.; Yokoyama, S. *ChemBioChem* **2006**, *7*, 134–139.
- (17) Gilmore, J. M.; Scheck, R. A.; Esser-Kahn, A. P.; Joshi, N. S.; Francis, M. B. *Angew. Chem., Int. Ed.* **2006**, *45*, 5307–5311.
- (18) Kodama, K.; Fukuzawa, S.; Nakayama, H.; Sakamoto, K.; Kigawa, T.; Yabuki, T.; Matsuda, N.; Shirouzu, M.; Takio, K.; Yokoyama, S.; Tachibana, K. *ChemBioChem* **2007**, *8*, 232–238.
- (19) Lin, Y. A.; Chalker, J. M.; Floyd, N.; Bernardes, G. J. L.; Davis, B. G. *J. Am. Chem. Soc.* **2008**, *130*, 9642–9643.
- (20) Chalker, J. M.; Wood, C. S. C.; Davis, B. G. *J. Am. Chem. Soc.* **2009**, *131*, 16346–16347.
- (21) Ho, C.-M.; Zhang, J.-L.; Zhou, C.-Y.; Chan, O.-Y.; Yan, J. J.; Zhang, F.-Y.; Huang, J.-S.; Che, C.-M. *J. Am. Chem. Soc.* **2010**, *132*, 1886–1894.
- (22) Höfle, G.; Steglich, W.; Vorbrüggen, H. *Angew. Chem., Int. Ed. Engl.* **1978**, *17*, 569–583.
- (23) Koshi, Y.; Nakata, E.; Miyagawa, M.; Tsukiji, S.; Ogawa, T.; Hamachi, I. *J. Am. Chem. Soc.* **2008**, *130*, 245–251.
- (24) Mammen, M.; Choi, S.-K.; Whitesides, G. M. *Angew. Chem., Int. Ed.* **1998**, *37*, 2754–2794.
- (25) Kiessling, L. L.; Gestwicki, J. E.; Strong, L. E. *Angew. Chem., Int. Ed.* **2006**, *45*, 2348–2368.
- (26) Muramoto, K.; Kagawa, D.; Sato, T.; Ogawa, T.; Nishida, Y.; Kamiya, H. *Comp. Biochem. Physiol. B* **1999**, *123*, 33–45.
- (27) Ladbury, J. E.; Lemmon, M. A.; Zhou, M.; Green, J.; Botfield, M. C.; Schlessinger, J. *Proc. Natl. Acad. Sci. U.S.A.* **1995**, *92*, 3199.
- (28) Clackson, T.; Yang, W.; Rozamus, L. W.; Hatada, M.; Amara, J. F.; Rollins, C. T.; Stevenson, L. F.; Magari, S. R.; Wood, S. A.; Courage, N. L.; Lu, X.; Cerasoli, F.; Gilman, M.; Holt, D. A. *Proc. Natl. Acad. Sci. U.S.A.* **1998**, *95*, 10437–10442.
- (29) Howl, J. *Peptides* **1999**, *20*, 515–518.
- (30) Marceau, F.; Hess, J. F.; Bachvarov, D. R. *Pharmacol. Rev.* **1998**, *50*, 357–386.
- (31) Langerström, M. C.; Schiöth, H. B. *Nat. Rev. Drug Discovery* **2008**, *7*, 339–357.
- (32) Koshi, Y.; Nakata, E.; Yamane, H.; Hamachi, I. *J. Am. Chem. Soc.* **2006**, *128*, 10413–10422.
- (33) Moore, A. F.; Fulton, R. W. *Drug Dev. Res.* **1984**, *4*, 331–349.
- (34) *Chem. Rev.* **2007**, *107* (12): Special issue on organocatalysis.
- (35) Ogawa, T.; Ishii, C.; Suda, Y.; Kamiya, H.; Muramoto, K. *Biosci. Biotechnol. Biochem.* **2002**, *66*, 476–480.
- (36) Nonaka, H.; Fujishima, S.; Uchinomiya, S.; Ojida, A.; Hamachi, I. *J. Am. Chem. Soc.* **2010**, *132*, 9301–9309.
- (37) Mori, Y.; Wakamori, M.; Miyakawa, T.; Hermosura, M.; Hara, Y.; Nishida, M.; Hirose, K.; Mizushima, A.; Kurosaki, M.; Mori, E.; Gotoh, K.; Okada, T.; Fleig, A.; Penner, R.; Iino, M.; Kurosaki, T. *J. Exp. Med.* **2002**, *195*, 673–681.